Volume 58(1): 17–28, 2010
Journal of Histochemistry & Cytochemistry
http://www.jhc.org

ARTICLE

Indoleamine 2,3-Dioxygenase Tissue Distribution and Cellular Localization in Mice: Implications for Its Biological Functions

Xiangchen Dai and Bao Ting Zhu

Department of Pharmacology, Toxicology, and Therapeutics, School of Medicine, University of Kansas Medical Center, Kansas City, Kansas

SUMMARY Earlier studies have suggested that indoleamine 2,3-dioxygenase (IDO) has a wide tissue distribution in mammals. However, detailed information on its cellular localization and also the levels of expression in various tissues is still scarce. In the present study, we sought to determine the cellular localization of IDO and also to quantify the level of its expression in various mouse tissues by using the branched DNA signal amplification assay, Western blotting, and immunohistochemical staining. The highest levels of constitutive IDO expression were found to be selectively present in the caput of epididymis, except for its initial segment. IDO expression was also detected inside the luminal compartment and even in the stereocilia within this region. In the prostate, high levels of IDO were selectively expressed in the capsular cells. In addition, high levels of IDO expression were also selectively detected in certain types of cells in the placenta, spleen, thymus, lung, and digestive tract. Notably, the morphological features of most of the positively stained cells in these organs closely resembled those of antigen-presenting cells. Based on the tissue distribution and cellular localization characteristics of IDO, it is hypothesized that its expression may serve two main functions: one is to deplete tryptophan in an enclosed microenvironment (such as in the epididymal duct lumen) to prevent bacterial or viral infection, and the other is to produce bioactive tryptophan catabolites that would serve to suppress T-cell–mediated immune responses against self-antigens, fetal antigens, or allogeneic antigens, in different situations.
(J Histochem Cytochem 58:17–28, 2010)

KEY WORDS
indoleamine 2,3-dioxygenase
cellular localization
tissue distribution
tryptophan catabolites
allograft tolerance

INDOLEAMINE 2,3-DIOXYGENASE (IDO, EC1.13.11.42), the rate-limiting enzyme of the kynurenine pathway, catalyzes the oxidative conversion of L-tryptophan to *N*-formylkynurenine (Hirata and Haysishi 1975; Shimizu et al. 1978). Studies in recent years have led to the suggestion that high levels of IDO expression in placental trophoblasts may play an important role in mediating the feto-maternal immune tolerance (Munn et al. 1998). In support of this hypothesis, it was shown that administration of 1-methyl-tryptophan, an inhibitor of IDO's catalytic activity, resulted in extensive inflammation, hemorrhagic necrosis, T-cell infiltration, and C3 deposition at the materno-fetal interface in mice, and ultimately the rejection of allogeneic fetuses (Mellor and Munn 2001). In addition, IDO expression in tumor cells has been suggested to contribute to inhibition of the cell-mediated anti-tumor immune response (Uyttenhove et al. 2003).

A number of studies in recent years have shown that the proliferating T-cells are important targets of IDO's immunosuppressive actions (Munn et al. 1999,2002; Dai and Zhu 2009). It was observed previously that increasing expression of IDO in macrophage-colony stimulating factor–derived macrophages or in monocyte-derived dendritic cells by treatment with interferon-γ resulted in strong inhibition of T-cell proliferation (Munn

Correspondence to: Bao Ting Zhu, Department of Pharmacology, Toxicology, and Therapeutics, University of Kansas Medical Center, MS-1018, room KLSIC-4061, 2146 W. 39th Ave., Kansas City, KS 66160. E-mail: btzhu@kumc.edu

Received for publication January 23, 2009; accepted August 20, 2009 [DOI: 10.1369/jhc.2009.953604].

et al. 2002). Similarly, high levels of IDO expression in human placental villous explants were also shown to inhibit T-cell proliferation (Munn et al. 2002). Two mechanisms have been suggested to account for the immunosuppressive actions of IDO: one is through tryptophan depletion (Munn et al. 1999) and the other is through the formation of bioactive tryptophan derivatives to exert immunosuppressive functions. In line with the tryptophan depletion hypothesis, studies have shown that cultured T-cells are arrested at the mid-G_1 point in the absence of tryptophan (Munn et al. 1999). However, it was recently shown that some of the tryptophan catabolites (such as 3-hydroxyanthranilic acid) formed by IDO could directly suppress T-cell response and immune rejection of cardiac allografts in vivo (Terness et al. 2002). This study, along with some of the earlier studies by others (Terness et al. 2002; Fallarino et al. 2003; Bauer et al. 2005; Funeshima et al. 2005), provided support for an alternative possibility that IDO may exert its immunosuppressive effect through the formation of bioactive tryptophan derivatives that suppress the T-cell–mediated immune response against allografts or self-antigens.

Because of the unique importance of IDO in modulating immune system functions as well as other biological processes, a number of earlier studies sought to determine its distribution in various tissues and cell types in the body. Earlier studies based on measuring enzyme activity in tissue homogenates reported the presence of IDO activity in epididymis, colon, intestine, cecum, thymus, trachea, lung, brain, spleen, and pancreas of animals (Yoshida et al. 1979), and its activity was also detected in some human tissues (Yamazaki et al. 1985). In addition, IDO was also found to be expressed in subsets of macrophages and dendritic cells in culture (Munn et al. 1999). However, detailed information on its cellular localization as well as its mRNA and protein levels in various tissues in vivo is still scarce, except for a few studies (Britan et al. 2006). In the present study, we have sought to characterize the tissue distribution and cellular localization of IDO and also to quantify its mRNA and protein expression levels in various mouse tissues by using the branched DNA (bDNA) signal amplification assay, Western blotting, and immunohistochemical staining. This information is of value in helping to formulate hypotheses concerning the physiological functions of IDO for further testing in animal models and also in humans.

Materials and Methods

Chemicals and Reagents

Horseradish peroxidase (HRP)-conjugated anti-rabbit IgG was purchased from Invitrogen (Carlsbad, CA), and HRP-conjugated anti-rat IgG2b was from Southern Biotech (Birmingham, AL). Anti–glyceraldehyde-3-phosphate dehydrogenase (GAPDH) antibodies were from Cell Signaling Technology (Danvers, MA). Chloroform, Tween-20, and Triton X-100 were from Fisher Scientific (Fair Lawn, NJ), and diaminobenzidine (DAB) was from Vector Laboratories (Burlingame, CA). The Bradford protein quantification assay kit and polyvinylidene difluoride (PVDF) membranes were purchased from BioRad (Hercules, CA). The enhanced chemiluminescence (ECL) detection system used in this study was a product of GE Healthcare (Buckinghamshire, UK).

The purified mIDO-48 monoclonal antibody used in the present study was obtained from Biolegend (San Diego, CA). The monoclonal antibody was raised against the recombinant mouse IDO protein. According to the supplier, this monoclonal antibody could selectively recognize the mouse IDO. In addition, Western blot analysis of various mouse tissues conducted in this study also confirmed that this antibody could selectively detect mouse IDO protein without appreciable crossreactivity with other mouse proteins. For instance, the Western blotting analysis showed that this antibody only produced a single band when liver whole homogenates were tested, suggesting that the antibody did not cross-react with the other isozymes present in liver, including the tryptophan dioxygenase, an enzyme that shares a high degree of sequence homology with IDO.

Animals and Tissue Preparation

Eight-week-old male and female C57BL/6J mice (five per group) were obtained from Harlan (Indianapolis, IN). The animal use procedures were approved by the Institutional Animal Care and Use Committee of the University of Kansas Medical Center, and the National Institutes of Health guidelines for the humane treatment of animals were strictly followed. The animals were sacrificed with CO_2 overdose followed by decapitation. Various tissues (kidney, bladder, urethra, prostate, testis, edididymis, ductus deferens, seminal vesicle, uterus, ovary, esophagus, stomach, duodenum, jejunum, ileum, colon, cecum, liver, pancreas, saliva gland, lung, heart, aorta, brain, spinal cord, eye, spleen, thymus, lymph node, adrenal gland, skin, and skeletal muscle) were collected, dissected, and washed in ice-cold phosphate-buffered saline (PBS), then processed immediately or frozen in liquid nitrogen, and stored at −80C until used in the experiments.

RNA Isolation and bDNA Signal Amplification Assay

Frozen tissues were homogenized in Trizol reagents (at 80 mg wet tissue/1 ml). Total RNA was isolated using the standard Trizol-chloroform-isopropylalcohol method. The total RNA concentration in each sample was quantified using a spectrophotometer (λ = 260 nm). The integrity of each RNA sample was evaluated using formaldehyde agarose gel electrophoresis before analysis. IDO mRNA was measured using the

bDNA signal amplification assay according to a method described previously (Hartley and Klaassen 2000). The mouse IDO gene sequence was obtained from the GenBank (accession no. M69109). Multiple oligonucleotide probe sets containing capture extenders, label extenders, and blockers (listed in Table 1) specific for a single mRNA transcript were designed using the ProbeDesigner software, version 1.0 (Bayer Corp.; Emeryville, CA). All probes were synthesized (50-nmol synthesis scale) by Integrated DNA Technologies (Coralville, IA), and were desalted and lyophilized. Total RNA (1 μg/1 μl) was added to each well (1 μg/well) of the 96-well plates containing 50 μl of capture hybridization buffer and 50 μl of diluted probe set. Total RNA was allowed to hybridize to the probe set overnight at 53C. Subsequent hybridization steps were carried out according to manufacturer-recommended protocols, and luminescence was measured with a Quantiplex 320 bDNA luminometer interfaced with Gen5 data management software (version 5.02). The intensity of luminescence for each well is reported as relative light units per 10 μg of total RNA.

Western Blotting

Tissues were homogenized in the radioimmunoprecipitation assay lysate buffer (consisting of 50 mM Tris-HCl, pH 7.4, 0.1 mM EDTA, 0.1% SDS, 0.15 M NaCl, 1% sodium deoxycholate, and protease inhibitors). After centrifugation at 10,000 × g for 10 min (at 4C), supernatants were collected. Protein concentrations were determined using a commercial kit based on the Bradford assay. Bovine serum albumin was used as standard. SDS-polyacrylamide gel electrophoresis (one-dimensional) was performed for separation of the proteins, and the gels were subsequently transferred onto Sequi-Blot PVDF membranes. The PVDF membranes were blocked in a buffered saline solution (0.05 M Tris-HCl and 0.2 M NaCl, pH 7.4) containing 0.1% (v/v) Tween (TBS with 0.5% bovine serum albumin) and 10% non-fat milk (w/v) for 1 hr at room temperature, and then incubated with the primary antibody [anti-IDO or anti-GAPDH antibody, diluted at 1:2000 in TBS with 10% Tween-20 (TBST) containing 10% non-fat milk] for 1 hr. The membranes were subsequently rinsed three times (10 min each) with TBST, incubated with HRP-conjugated anti-rat IgG2b or HRP-conjugated anti-rabbit IgG, respectively, for 1 hr at room temperature, and then rinsed three times with TBST (10 min each). Secondary antibodies on the membranes were detected with an ECL detection system. The densitometry of the detected protein bands was determined using the Scion image analysis software. The densitometry ratio of IDO protein to GAPDH protein was calculated. For the purpose of comparison between different tissues and between different sets of experiments, the densitometry ratio for each tissue was normalized to the densitometry ratio measured for epididymis, which was determined in each experiment as a control.

Immunohistochemical Staining

Organs were dissected and fixed in 10% (w/v) neutral buffered formalin for 24 hr. Formalin-fixed tissues were processed into paraffin and cut into 5-μm sections on plain slides. Slides were dried for 45 min at 45C, dewaxed in xylene, and rehydrated through ethanol-graded solutions to water. Slides were immersed in citritic buffer solution (pH 6.0) and boiled in a microwave oven for 15 min to retrieve antigens. Endogenous peroxidase was quenched with 3% H_2O_2 in PBS for 30 min. Slides were blocked for 1 hr with 5% normal serum from the same species in which the secondary antibody was made. The primary antibody (rat anti-

Table 1 Oligonucleotide probes generated for analysis of mouse IDO mRNA expression by QuantiGene branched DNA signal amplification assay

Name	Target region	Function	Sequence
mIDO001	194046:71-1294.243.259.CE	CE	gggccaggtgtgccaggTTTTTctcttggaaagaaagt
mIDO002	194046:71-1294.321.339.CE	CE	aacagcaatattgcggggcTTTTTctcttggaaagaaagt
mIDO003	194046:71-1294.405.425.CE	CE	tccttttttcttccagtttgccTTTTTctcttggaaagaaagt
mIDO004	194046:71-1294.530.551.CE	CE	gctttgattgcaggagaagctgTTTTTctcttggaaagaaagt
mIDO005	194046:71-1294.219.242.LE	LE	cgctgtaacctgtgtcctctcagtTTTTTaggcataggacccgtgtct
mIDO006	194046:71-1294.260.279.LE	LE	cgccatggtgatgtaccccaTTTTTaggcataggacccgtgtct
mIDO007	194046:71-1294.280.299.LE	LE	tcccctcggttccacacataTTTTTaggcataggacccgtgtct
mIDO008	194046:71-1294.300.320.LE	LE	agcacctttcgaacatcgtcaTTTTTaggcataggacccgtgtct
mIDO009	194046:71-1294.340.360.LE	LE	ctctgagagctcgcagtagggTTTTTaggcataggacccgtgtct
mIDO010	194046:71-1294.361.379.LE	LE	taggaggcaggcccaacttTTTTTaggcataggacccgtgtct
mIDO011	194046:71-1294.380.404.LE	LE	aggacacagtctgcataagacagaaTTTTTaggcataggacccgtgtct
mIDO012	194046:71-1294.442.466.LE	LE	acagaatgtccatgttctcgtatgtTTTTTaggcataggacccgtgtct
mIDO013	194046:71-1294.507.529.LE	LE	cgatttccaccaatagagagacgTTTTTaggcataggacccgtgtct
mIDO014	194046:71-1294.426.441.BL	BL	catgggcccattgggg
mIDO015	194046:71-1294.467.487.BL	BL	agtccccaccaggaaatgaga
mIDO016	194046:71-1294.488.506.BL	BL	aggaagaagcccttgtcgc

CE, capture extender; LE, label extender; BL, blocker.

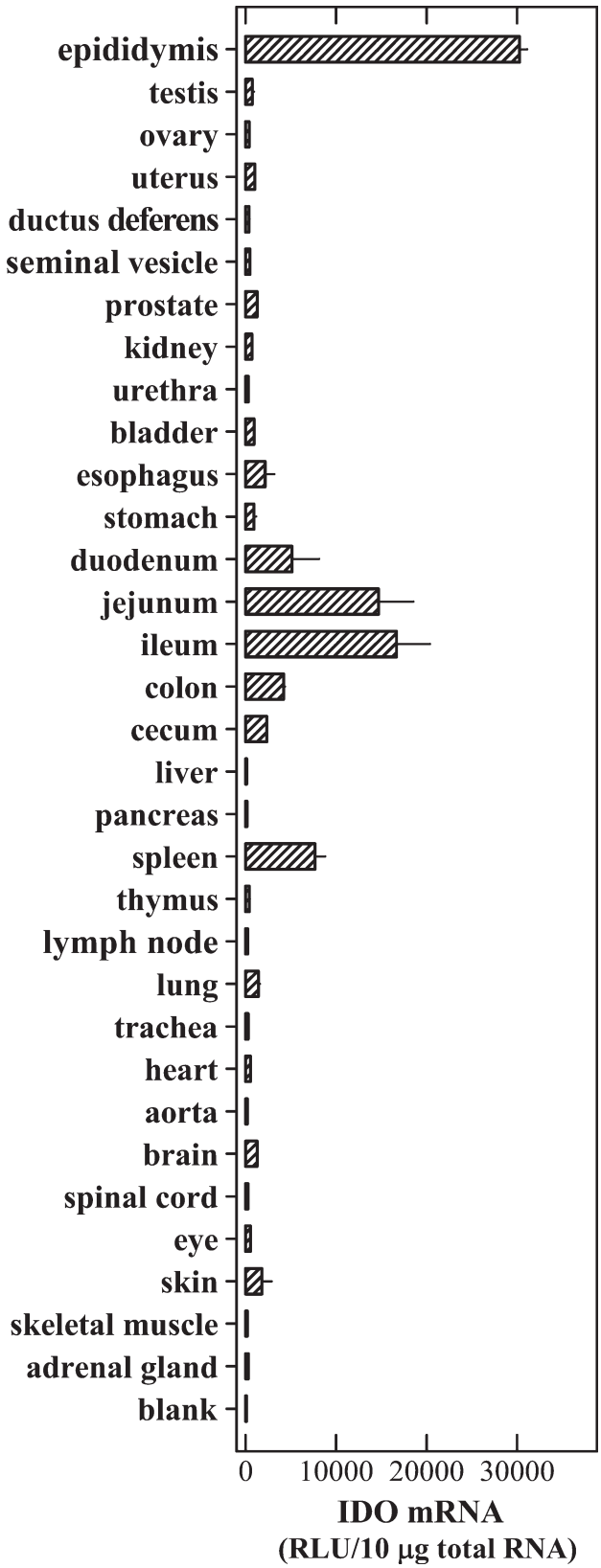

Figure 1 Levels of indoleamine 2,3-dioxygenase (IDO) mRNA in various mouse tissues. The procedures for the collection of tissues and for the branched DNA signal amplification assay are described in detail in Materials and Methods. Each value is the mean ± SD of triplicate determinations. Two separate experiments were conducted, and similar data were obtained (one representative data set is shown).

mouse IDO antibody) was diluted (at 1:100, v/v) in PBS with 0.1% Tween-20 before use and incubated for 1 hr at room temperature. For isotype control, the secondary antibody (HRP-conjugated anti-rat IgG2b antibody, diluted at 1:1000, v/v) was incubated for 1 hr. DAB was used as chromogen. Tissue sections were counterstained with hematoxylin QS, mounted in the mounting medium, and visualized under a light microscope. The immunohistochemical images were taken using an Olympus light microscope equipped with a CCD camera (DP70, Olympus).

Results

Levels of IDO mRNA Transcripts in Mouse Tissues

An elegant earlier study showed that the IDO mRNA was detected in mouse epididymis, prostate, lung, smooth muscle, and heart, with highest levels found in epididymis but much lower levels in other tissues (Britan et al. 2006). In this study, we further compared the constitutive IDO mRNA levels in a larger number of mouse tissues by using the bDNA signal amplification assay (data summarized in Figure 1). Of all tissues tested, highest levels of IDO mRNA were consistently detected in epididymis. Although the IDO mRNA levels were generally much lower in other tissues of the male genitourinary system compared with epididymis, IDO expression could still be readily detected in the prostate, bladder, and kidney. In female mice, IDO mRNA was also readily detected in the uterus. In the immune system, high levels of IDO mRNA were detected in the spleen, and relatively lower levels were detected in thymus and lymph nodes. Most regions of the gastrointestinal tract (such as esophagus, stomach, duodenum, jejunum, ileum, colon, and cecum) expressed readily detectable levels of IDO mRNA. It is of interest to note that the small intestine (particularly the ileum and jejunum) expressed very high levels of IDO mRNA. In comparison, IDO mRNA levels in liver and pancreas, two solid organs of the digestive system, were barely detectable. The levels of IDO mRNA in lung, brain, skin, heart, and eye were also detected, albeit at rather low levels. Little IDO expression was detected in other tissues, such as trachea, aorta, spinal cord, and skeletal muscle.

Levels of IDO Protein in Mouse Tissues

There is little information available in the literature concerning IDO protein levels in various tissues. Therefore, we sought to determine in this study the IDO protein levels by using Western blot analysis (data are shown

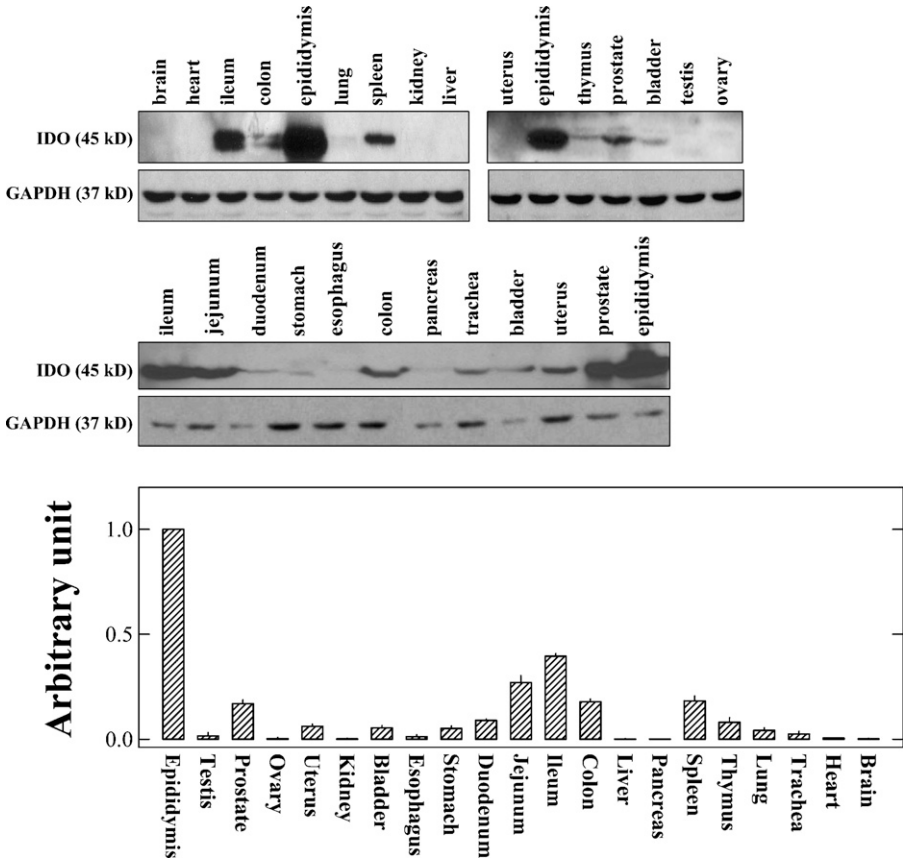

Figure 2 Levels of IDO protein in various mouse tissues determined by Western blot analysis. The upper panel shows the representative IDO bands for different tissue samples detected by Western blotting, and the lower panel shows the quantitative comparison of IDO protein levels in different tissues based on densitometry measurements. The procedures for the collection of tissues and for the Western blotting analysis are described in detail in Materials and Methods. Note that for most tissues, the analysis was conducted multiple times. In each experiment, the proteins from pooled epididymis tissue were included as a control for comparison. The relative levels of IDO protein in each tissue are expressed as a relative unit that considers the IDO protein level in epidydymis to be 100%. Each value is the mean ± SD of at least three experiments.

in Figure 2, upper panel). Note that only those tissues that were found to have detectable levels of IDO mRNA transcripts (described above; Figure 1) were selected for further determination of its protein levels. For most of the tissues tested, a protein band with a size of ~45 kDa was selectively detected, which corresponds to the known size of mouse IDO protein.

The relative levels of IDO protein in different tissues were calculated according to densitometry measurements, and the data are summarized in Figure 2 (lower panel). The highest levels of IDO protein were consistently detected in epididymis, which agrees with IDO mRNA data. Although IDO mRNA levels were relatively low in prostate and bladder, rather high levels of IDO protein were detected in these two tissues. In the digestive system, ileum, jejunum, and colon were found to have high levels of IDO protein, consistent with the mRNA data. IDO protein was also detected in the spleen, thymus, trachea, and lung. In the testis and ovary, IDO protein levels were very low.

Immunohistochemical Localization of IDO-expressing Cells in Mouse Tissues

Genitourinary System. Strong staining of IDO-positive cells was detected in a number of tissues of the genitourinary system. Nearly all columnar epithelial cells (apical cells) in the caput of epididymis (except the initial segment), including their stereocilia, which are in the lumen, were strongly and selectively stained positive for IDO (Figures 3A, 3B, and 3C). It was suggested in an earlier study that IDO immunoreactivity was mostly present in the basal half of most apical epithelial cells but essentially absent in the upper half bordering the epididymal duct lumen, and that no IDO staining was present inside the lumen (Britan et al. 2006). However, the data from the study showed that IDO-positive staining was present throughout the cells, and, interestingly, it appeared that even heavier staining was observed for the bundled stereocilia, which were found inside the epididymal duct lumen (Figure 3E). To compare IDO staining intensity in apical epithelial cell bodies with their stereocilia in the lumen, we chose to incubate the tissue slides with DAB for a shorter period of time. Under this detection condition, we could clearly see that stereocilia had a far stronger staining of IDO than did their cell bodies (Figure 3F). This observation suggests that IDO that is synthesized in the apical epithelial cells may be mostly translocated to the stereocilia. Furthermore, it is evident that the spermatozoa inside the lumen were essentially not stained (Figure 3F). Interestingly, nearly all epithelial

The Journal of Histochemistry & Cytochemistry

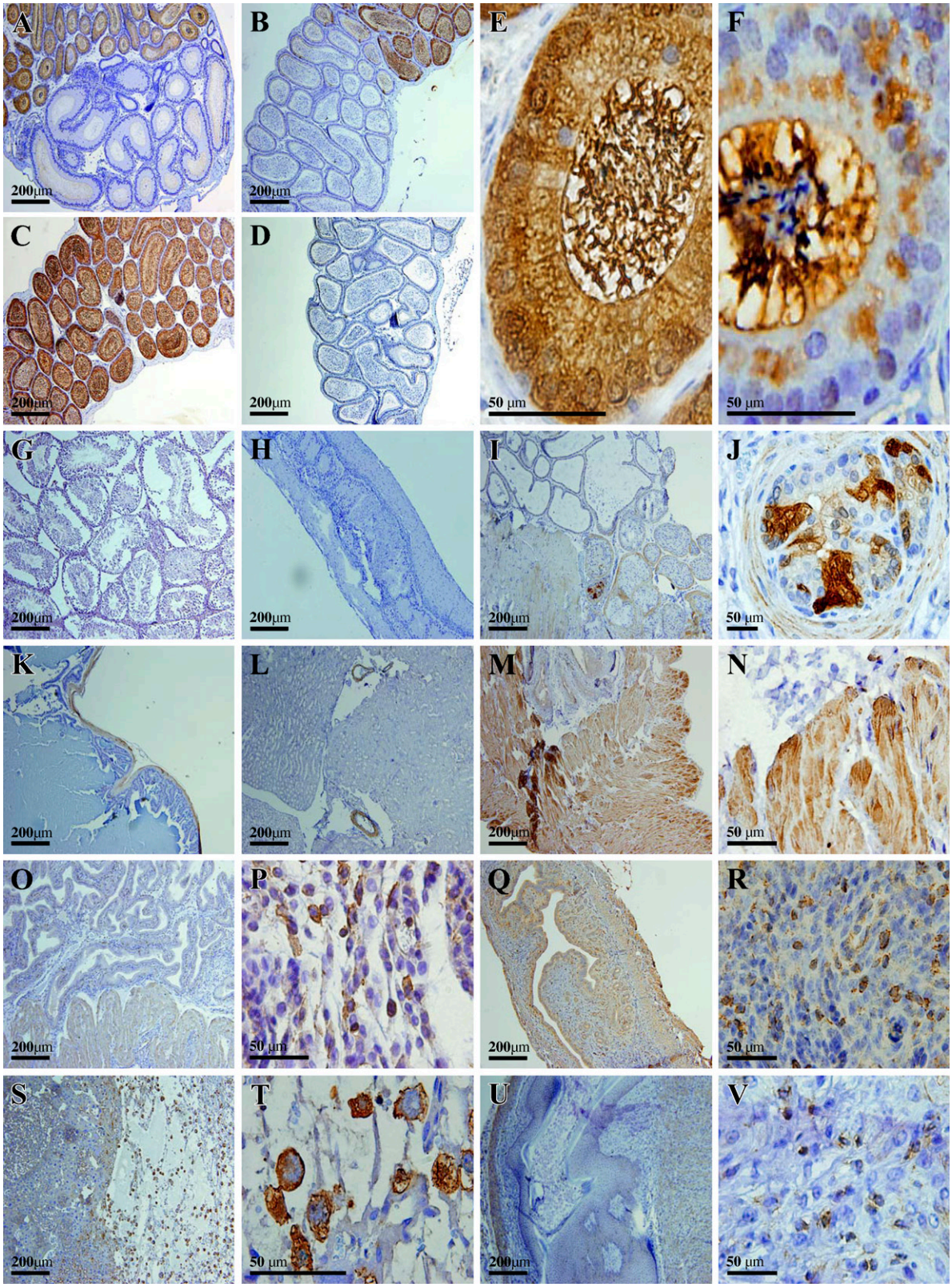

cells in the initial segment of the caput (Figure 3A), and those in the corpus (Figure 3B) and cauda regions (Figure 3D), were completely and selectively devoid of any IDO immunoreactivity. In addition, IDO was not detected in testis (Figure 3G), ductus deferens (Figure 3H), and seminal vesicle (Figure 3K).

In the prostate, cells with strong IDO staining were detected mostly in the capsular smooth-muscle fibers (Figure 3I), as well as in some of the epithelial cells (Figure 3J). Cells in other parts of the prostate glands were essentially not stained for IDO. In the kidney from male or female mice, the positive staining was only localized to the smooth-muscle layer of the small blood vessels, whereas the vascular endothelial cells were not stained (Figure 3L). In the bladders from both genders, IDO-positive cells were mostly found in the muscularis layer (Figure 3M), and basically no appreciable staining was present in the mucosa layer (Figure 3N).

In the uterus of female mice, IDO-positive cells were present in the endometrium and myometrium during the secretory phase (Figure 3O). Cells with strong IDO-positive staining were scattered all over the endometrial layer, and most of them were located immediately underneath the endometrial lining (Figure 3P). These IDO-positive cells appeared to resemble macrophages. In addition, moderate levels of IDO immunoreactivity were widely distributed within the myometrium. By contrast, few IDO-positive cells were detected in the uterus during the proliferative phase, particularly the endometrium (data not shown). Large numbers of IDO-positive cells were detected in the uterus on the 9th day of pregnancy (Figures 3Q and 3R). In the placenta, IDO cells were strongly detected in syncytiotrophoblasts (Figure 3S), with a predominant cytosolic localization (Figure 3T). In the ovary, IDO staining was either very weak or mostly absent. Those cells with detectable levels of IDO staining were mostly smooth-muscle fibers in the medulla and tunica albuginea (data not shown).

Digestive System. Although cells with strong IDO immunreactivity were readily detected along the gastrointestinal (GI) tract, the small intestine had the highest levels of IDO expression. In duodenum, positive staining was detected in the lamina propria of villi and also in the glands (Figures 4C and 4D). In jejunum and ileum, IDO-positive staining was mostly detected within the interstitial space of the villi or the mucosa layer (Figures 4E and 4F). These cells had an appearance resembling macrophages and dendritic cells, which are required for antigen processing and presentation. Subcellularly, IDO had an exclusive cytosolic or perinuclear localization. Notably, IDO-positive cells were essentially absent in the epithelial lining (including goblet cells).

Peyer's patches were also found to be strongly stained for IDO (Figure 4K). Peyer's patches are lymphoid aggregations within the lamina propria, and IDO-positive cells in this lymphoid structure are thought to play an important role as modulators of the intestinal immune responses.

In colon and cecum, IDO-positive cells were mainly detected in connective tissues between the glands that occupied the lamina propria of the mucosa (Figures 4G and 4H). These connective tissues usually contain a network of capillaries and a number of cell types such as lymphocytes, plasma cells, macrophages, fibroblasts, and smooth-muscle cells. Based on the morphology, IDO-positive cells were relatively large in size and irregular in shape, with a gross appearance resembling macrophages.

Cells with IDO-positive staining were also detected in the mucosa of the stomach (Figure 4B), although the levels of its mRNA were very low. According to mRNA detection results, the esophagus expressed relatively high levels of IDO. Although no significant staining was detected in mucosal cells of the esophagus, weak staining was detected in the smooth-muscle cells (Figure 4A).

At present, there is little information available concerning IDO expression in the pancreas. Our data showed that constitutive IDO expression was found mostly in the blood vessel walls in this tissue (Figure 4I). In addition, IDO-positive cells were detected in the Islets of Langerhans, which consist mostly of cells that secrete insulin as well as some of the other peptide hormones.

Basically, no positive staining was found in the liver (Figure 4J), which is consistent with a previous report (Hansen et al. 2004). The lack of IDO immune reactivity in the liver, in turn, indicates that the antibody used in the present study did not crossreact with tryptophan dioxygenase, an enzyme that is closely related to IDO (with a high degree of sequence homology between these two enzymes).

Immune System. It was reported earlier that very few cells in the spleen of untreated control mice expressed

Figure 3 Immunohistochemical localization of IDO protein in the mouse genitourinary system. **(A)** Initial and second segments of the caput of epididymis. **(B)** Last segment of the caput and corpus of epididymis. **(C)** Caput of epididymis (not including the initial segment). **(D)** Cauda of epididymis. **(E)** High magnification showing the stained cells in the caput of epididymis. **(F)** High magnification of stained cells in the caput of epididymis. Note that in this experiment, incubation of the tissue slides with DAB lasted for a shorter length of time than usual. **(G)** Testis; **(H)** ductus deferens; **(I,J)** prostate; **(K)** seminal vesicle; **(L)** kidney; **(M,N)** bladder; **(O,P)** uterus in the secretory phase; **(Q,R)** uterus (9th day of pregnancy); **(S,T)** placenta; **(U,V)** ovary.

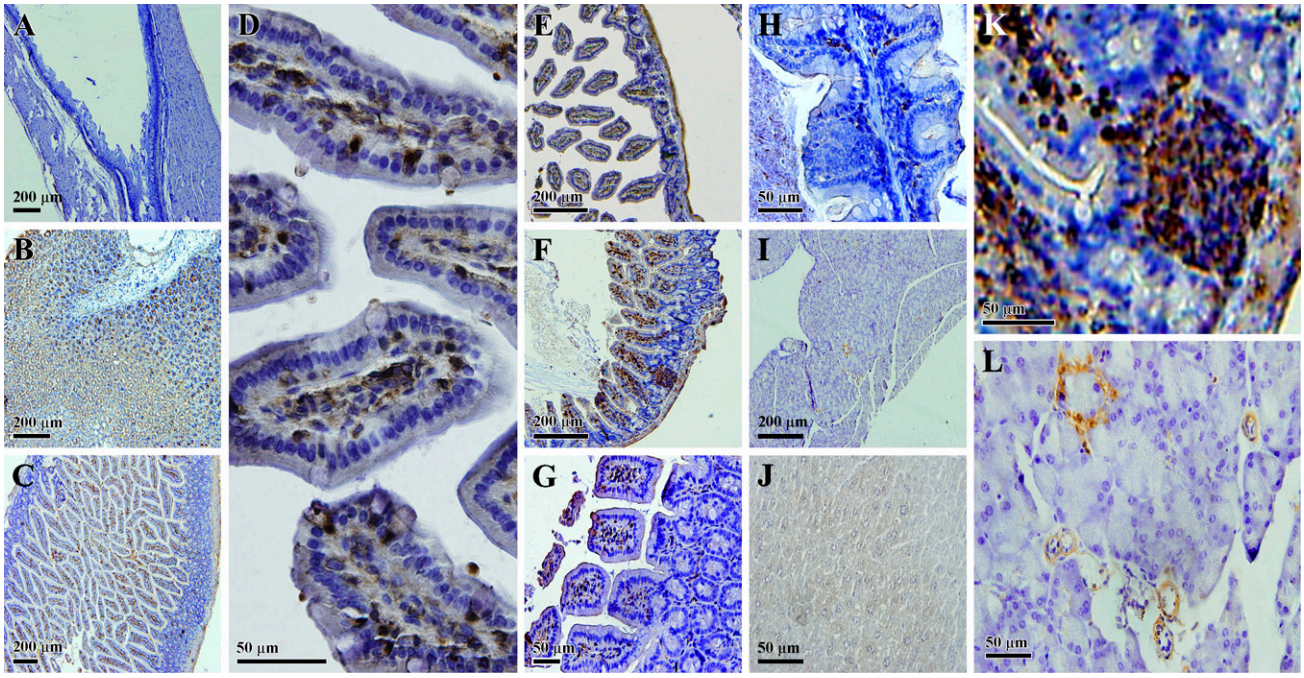

Figure 4 Immunohistochemical localization of the IDO protein in the mouse digestive system. **(A)** Esophagus; **(B)** stomach; **(C,D)** low and high magnification, respectively, of stained cells in the duodenum; **(E)** jejunum; **(F)** ileum; **(G)** colon; **(H)** cecum; **(I)** pancreas; **(J)** liver; **(K)** high magnification of stained cells in the ileum; **(L)** high magnification of stained cells in the pancreas.

IDO, and clusters of IDO-positive cells were mostly small mononuclear cells dispersed throughout splenic red pulp areas (Mellor et al. 2003). The results of this study showed that IDO-positive cells were mostly scattered in the red pulp area, particularly in the marginal zone (Figure 5A). The marginal zone is an area between the white pulp and the surrounding red pulp, and contains macrophages and reticular cells (with antigen-presenting functions) but relatively few lymphocytes. With regard to the cell types, we believe reticular cells in this region are the major type of cells that were positively stained for IDO (Figure 5B).

In the thymus, cells with relatively weak IDO immunoreactivity were present in the cortex, but stronger staining was mostly concentrated in the medulla zone (Figure 5C), which is composed of macrophages, loosely packed lymphocytes, and also eosinophils. It appeared that macrophages were among the major types of cells stained in the medulla zone of thymus (Figure 5D).

In the lymph nodes, two very different staining patterns were observed. In axillary lymph nodes, we could hardly detect any cells that were stained positively for IDO (Figures 5E and 5F), whereas in jugular lymph nodes, IDO-positive cells were readily detected throughout the cortex and medulla (Figure 5G). The staining was localized to the cytoplasmic compartment (Figure 5H). The observed difference in the distribution of IDO-positive cells in axillary and vertical lymph nodes was rather interesting, and might reflect their distinct roles in mediating different types of immune responses.

Other Organs and Tissues. IDO expression was also reported previously to be present in lung interstitial antigen-presenting cells (Swanson et al. 2004). We found that IDO-positive cells in this organ included mostly interstitial cells (Figure 5I). Moreover, some smooth-muscle cells of the intrapulmonary bronchus also appeared to be positively stained (Figure 5J). No appreciable staining was detected in the trachea (Figure 5K). In the thyroid gland, IDO was weakly stained in the epithelium (Figure 5L). In the heart, IDO was mainly expressed in blood vessels and also weakly stained in heart muscle cells (Figures 5M and 5N). In the central nervous system (CNS), it was reported that IDO immunoreactivity was localized in neurons of the hippocampus (Roy et al. 2005). Notably, two recent studies reported little or no IDO expression in the CNS except after meningitis or cortical lesions (Kwidzinski et al. 2003) or following malaria infection (Hansen et al. 2004). We found a rather clear IDO staining in the regions surrounding the cerebral cavities (Figure 5O). In the adrenal glands, weak staining was detected in the cortex (Figure 5P). In the skeletal muscle, IDO staining was mainly seen in the blood vessels (Figures 5U and 5V). In the skin, Langerhans cells were selectively stained (Figures 5W and 5X). In the eye, positive IDO staining was detected in the corneal epithelium

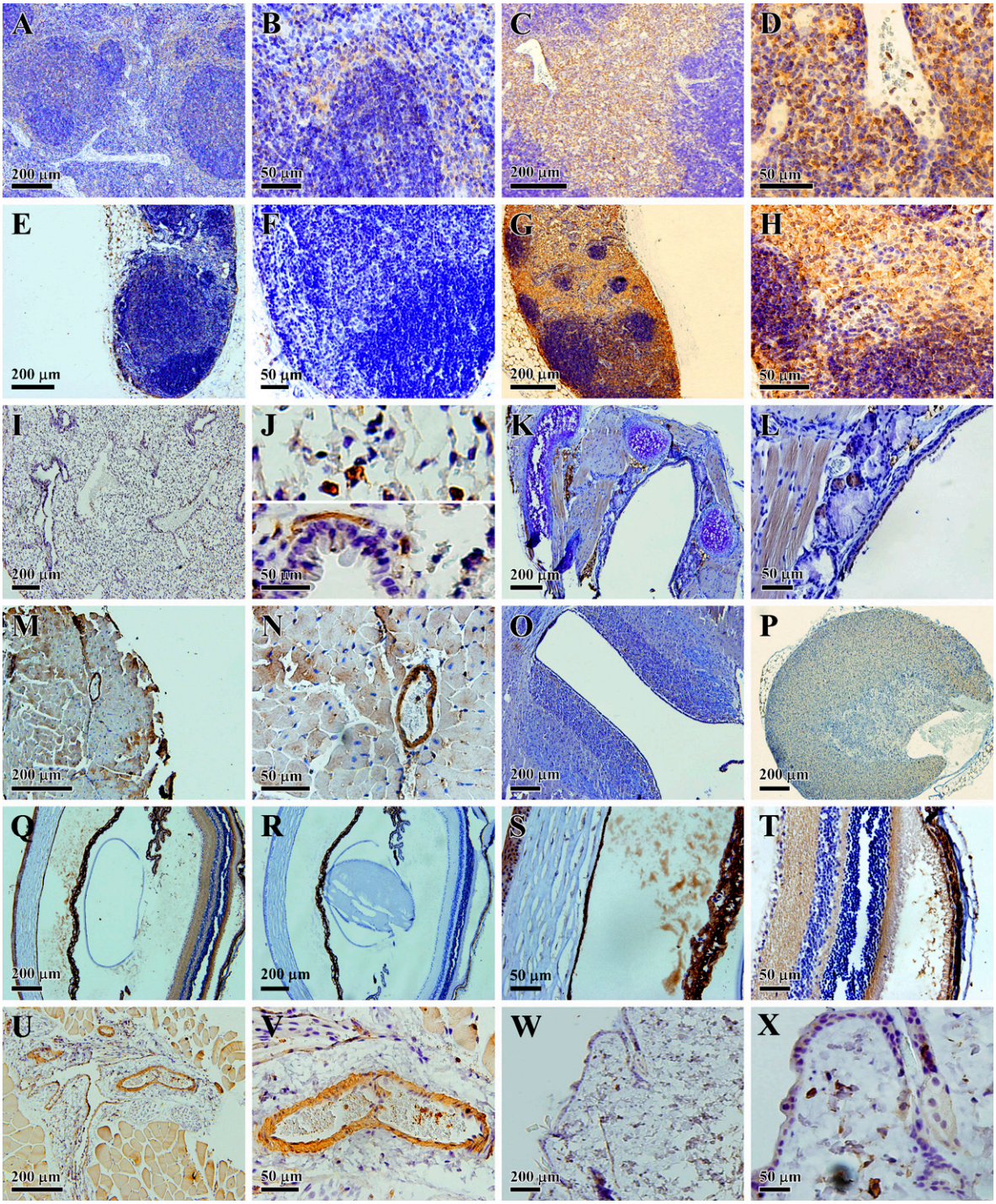

Figure 5 Immunohistochemical localization of IDO protein in other mouse systems. (**A,B**) Low and high magnification, respectively, of stained cells in the spleen. (**C,D**) Low and high magnification, respectively, of stained cells in the thymus. (**E,F**) Low and high magnification, respectively, of an axillary lymph node. (**G,H**) Low and high magnification, respectively, of stained cells in a jugular lymph node. (**I,J**) Low and high magnification, respectively, of stained cells in the lung. (**K**) Trachea. (**L**) Thyroid. (**M,N**) Low and high magnification, respectively, of stained cells in the heart. (**O**) Brain. (**P**) Adrenal gland. (**Q**) Low magnification of stained cells in the eye. (**R**) Low magnification of cells in the eye with negative staining. (**S,T**) High magnification of stained cells in the eye. (**U,V**) Low and high magnification, respectively, of stained cells in the skeletal muscle. (**W,X**) Low and high magnification, respectively, of stained cells in the skin.

The Journal of Histochemistry & Cytochemistry

and endothelium (Figure 5Q), when the overall staining pattern was compared against the negative control staining in the absence of IDO antibody (Figure 5R). In the anterior chamber of the eye, there was also obvious IDO staining (Figure 5S). In addition, there was strong positive staining in the outer limiting membrane, outer plexiform layer, and inner plexiform layer of the retina (Figure 5T).

Discussion

Characteristics of IDO Tissue Distribution and Possible Implications for Its Biological Functions in Representative Tissues

Epididymis and Prostate. Based on the data from earlier studies (Britan et al. 2006), as well as data from this study, a clear feature of IDO distribution in the caput of epididymis is that there is a clear-cut, segregated region where epithelial cells uniformly express very high levels of IDO protein, whereas the epithelial cells immediately next to the positively stained caput region are completely devoid of any detectable IDO staining. This unique pattern of segregated localization is really intriguing, and may be associated with its distinct, region-specific biological functions. On the basis of the unusually high levels of IDO expression in all apical epithelial cells (including their stereocilia) in this region, it is suggested that IDO can readily and completely deplete tryptophan inside the epididymal ducts of the caput. This depletion may serve the function of preventing bacterial and viral infections by suppressing the proliferation of bacteria and virus. It is known that epididymitis is the most common cause of intrascrotal inflammation, which is most often caused by a secondary bacterial infection of the lower the urinary tract. It appears highly probable that the selective expression of IDO in the caput of epididymis may provide a segregated region of tryptophan depletion that would effectively suppress the spread of local bacterial or viral infections along the seminiferous tubules, where vitally important spermatogenesis takes place.

A similar example was seen in the prostate gland, where cells with heavy IDO staining were detected almost exclusively in smooth-muscle fibers and in some of the epithelial cells of a dense connective tissue capsule that encapsulates the prostate gland. It is possible that the highly localized strong IDO staining in prostate capasular cells may also be related to reducing local inflammation by suppressing the proliferation of pathogenic microorganisms (e.g., bacteria and viruses) through tryptophan depletion.

Placenta. Data from earlier studies (Yamazaki et al. 1985; Munn et al. 1998; Mellor and Munn 2001; Sedlmayr et al. 2002), as well as data from this study, showed that very high levels of IDO immunostaining were found to be selectively present in placental syncytiotrophobasts. It is widely thought that tryptophan depletion may contribute as a main mechanism for IDO's immunosuppressive effect. However, other possible alternatives should also be considered for the following reasons: First, for tryptophan depletion to be a viable mechanism responsible for IDO-induced T-cell suppression in vivo, it is likely that the concentrations of tryptophan would have to be maintained at very low levels (probably <0.5–1 μM) for a long period of time in this microenvironment. However, the plasma levels of tryptophan are usually in the range of 60–80 μM; moreover, it is likely that the rate of diffusion of tryptophan into the placenta is much faster than the rate of its local degradation (considering the rapid supply through circulation). Consequently, it would seem rather difficult for tryptophan depletion to work effectively as a viable mechanism for immunosuppression. Second, it is known that the placenta is an organ that supplies nutrients to the fetus, and it would also seem rather inconceivable that most or all of the tryptophan (an essential amino acid) that circulates to the placenta is degraded by the placental IDO.

An alternative possibility is that the placental syncytiotrophobasts, which are in direct contact with the maternal immune system, may produce certain tryptophan catabolites (catalyzed by IDO along with other enzymes) to inhibit T-cell proliferation and to effectively suppress unwanted T-cell responses against fetal tissues. Because the formation of adequate amounts of immunosuppressive tryptophan catabolites may not require the depletion of the entire placental pool of tryptophan, this probably would not deprive the placenta of sufficient tryptophan for fetal growth.

Immune System. Morphologically, most of the IDO-positive cells observed in various lymph tissues appear to resemble various types of antigen-presenting cells (e.g., dendritic cells, macrophages, and reticular cells). Hence, it is suggested that localized formation of certain tryptophan catabolites by IDO, along with other enzymes present in various antigen-presenting cells, may serve to inhibit T-cell–mediated immune responses against self-antigens, fetal antigens, or allogeneic antigens. In this context, it is also of note that because many types of cancer cells expressed elevated levels of IDO, this is probably also a viable mechanism used by cancer cells to effectively evade T-cell–mediated autoimmune attacks. In support of this hypothesis, a recent study showed that 3-hydroxyanthranic acid, one of the tryptophan catabolites, could suppress the immune rejection of cardiac allografts in a rat model, and this effect was associated with a strong suppression of donor-specific dendritic cell-induced T-cell proliferation (Dai and Zhu 2009).

GI Tract. A majority of cells in the Peyer's patches were found to be strongly stained for IDO. Peyer's patches are lymphoid aggregations within the lamina propria. IDO-positive cells in this lymphoid structure are thought to be closely related to its suggested role as modulator of intestinal immune responses. On the basis of the localization, and also of morphological features of IDO-positive cells throughout the GI tract, it is suggested the IDO-positive cells are mostly antigen-presenting cells, and probably responsible for suppressing aberrant T-cell responses against food-borne cellular or non-cellular immunogens, and ultimately avoiding aberrant autoimmune responses against host tissues (as a result of crossreactivity).

Other Organs or Tissues. In the eye, positive IDO staining was detected in the corneal epithelium and, in mice, the anterior chamber. IDO activity was previously detected in rabbit eyes and was particularly elevated in the iris/ciliary body (Chiarugi et al. 1999). An earlier study also showed that although low levels of IDO mRNA and protein were detected in normal cornea, IDO expression was significantly increased following corneal transplantation. Following IDO cDNA transfer, murine corneal endothelial cells expressed functional IDO, which was effective in inhibiting allogeneic T-cell proliferation, and also prolonged the survival of corneal allografts (Beutelspacher et al. 2006). In addition, strong positive staining was detected in the outer limiting membrane, outer plexiform layer, and inner plexiform layer of the retina. The high IDO levels in these cells probably suggest that tryptophan catabolites may also play an important role in the development and maintenance of self-tolerance to immunologically privileged retinal antigens.

Given the fact that pancreatic islet cells are susceptible to pathogenic autoimmune attacks in type I diabetic patients, it is tempting to suggest the possibility that inadequate IDO expression in the Islets of Langerhans may constitute an endogenous risk factor predisposing the islet cells to aberrant autoimmune attacks. It will be of interest in the future to determine whether low levels of constitutive IDO expression in pancreatic islet cells constitute an etiological factor that increases the susceptibility to type I diabetes.

Conclusions and Clinical Implications

Based on the tissue distribution and cellular localization data obtained in this study, it is hypothesized that localized IDO expression may have two main biological functions: one is to deplete tryptophan in isolated microenvironments (such as in the epididymal duct lumen) to prevent bacterial or viral infection, and the other is to produce bioactive tryptophan catabolites to suppress T-cell–mediated immune responses. Regarding the latter, it is suggested that local formation of certain tryptophan catabolites, but not complete depletion of tryptophan by IDO, together with other enzymes present in antigen-presenting cells (e.g., dendritic cells, macrophages, reticular cells, and placental syncytiotrophoblasts) may serve to inhibit the T-cell–mediated immune rejection against self-antigens, fetal antigens, or allogeneic antigens. This hypothesis is partially supported by recent data showing that certain tryptophan catabolites can strongly suppress the T-cell–mediated autoimmune response against cardiac allografts in vivo (Dai and Zhu 2009). In this context, it is also of note that because many types of cancer cells express elevated levels of IDO, this is probably one of the mechanisms used by cancer cells to evade T-cell–mediated immune surveillance. More studies are warranted to further test these hypotheses.

Acknowledgments

The Quantiplex 320 bDNA luminometer interfaced with Gen5 data management software (version 5.02) is part of a core facility that is supported in part by National Institutes of Health Grant P20RR021940 from the National Center for Research Resources.

The authors thank Dr. Hong Lu at the University of Kansas Medical Center for technical assistance with the bDNA assay of the IDO mRNA present in various mouse tissues.

Literature Cited

Bauer TM, Jiga LP, Chuang JJ, Randazzo M, Opelz G, Terness P (2005) Studying the immunosuppressive role of indoleamine 2,3-dioxygenase: tryptophan metabolites suppress rat allogeneic T-cell responses in vitro and in vivo. Transpl Int 18:95–100

Beutelspacher SC, Pillai R, Watson MP, Tan PH, Tsang J, McClure MO, George AJ, et al. (2006) Function of indoleamine 2,3-dioxygenase in corneal allograft rejection and prolongation of allograft survival by over-expression. Eur J Immunol 36:690–700

Britan A, Maffre V, Tone S, Drevet JR (2006) Quantitative and spatial differences in the expression of tryptophan-metabolizing enzymes in mouse epididymis. Cell Tissue Res 324:301–310

Chiarugi A, Rapizzi E, Moroni F, Moroni F (1999) The kynurenine metabolic pathway in the eye: studies on 3-hydroxykynurenine, a putative cataractogenic compound. FEBS Lett 453:197–200

Dai X, Zhu BT (2009) Suppression of T-cell response and prolongation of allograft survival in a rat model by tryptophan catabolites. Eur J Pharmacol 606:225–232

Fallarino F, Grohmann U, Vacca C, Orabona C, Spreca A, Fioretti MC, Puccetti P (2003) T cell apoptosis by kynurenines. Adv Exp Med Biol 527:183–190

Funeshima N, Fujino M, Kitazawa Y, Hara Y, Hayakawa K, Okuyama T, Kimura H, et al. (2005) Inhibition of allogeneic T-cell responses by dendritic cells expressing transduced indoleamine 2,3-dioxygenase. J Gene Med 7:565–575

Hansen AM, Ball HJ, Mitchell AJ, Miu J, Takikawa O, Hunt NH (2004) Increased expression of indoleamine 2,3-dioxygenase in murine malaria infection is predominantly localized to the vascular endothelium. Int J Parasitol 34:1309–1319

Hartley DP, Klaassen CD (2000) Detection of chemical-induced differential expression of rat hepatic cytochrome P450 mRNA transcripts using branched DNA signal amplification technology. Drug Metab Dispos 28:608–616

Hirata F, Haysishi O (1975) Studies on indoleamine 2,3-dioxygenase: superoxide anion as substrate. Biochem J 250:5960–5966

Kwidzinski E, Bunse J, Kovac AD, Ullrich O, Zipp F, Nitsch R,

Bechmann I (2003) IDO (indolamine 2,3-dioxygenase) expression and function in the CNS. Adv Exp Med Biol 527:113–118
Mellor AL, Baban B, Chandler P, Marshall B, Jhaver K, Hansen A, Koni PA, et al. (2003) Cutting edge: induced indoleamine 2,3-dioxygenase expression in dendritic cell subsets suppresses T cell clonal expansion. J Immunol 171:1652–1655
Mellor AL, Munn DH (2001) Tryptophan catabolism prevents maternal T cells from activating lethal anti-fetal immune responses. J Reprod Immunol 52:5–13
Munn DH, Shafizadeh E, Attwood JT, Bondarev I, Pashine A, Mellor AL (1999) Inhibition of T cell proliferation by macrophage tryptophan catabolism. J Exp Med 189:1363–1372
Munn DH, Sharma MD, Lee JR, Jhaver KG, Johnson TS, Keskin DB, Marshall B, et al. (2002) Potential regulatory function of human dendritic cells expressing indoleamine 2,3-dioxygenase. Science 297:1867–1870
Munn DH, Zhou M, Attwood JT, Bondarev I, Conway SJ, Marshall B, Brown C, et al. (1998) Prevention of allogeneic fetal rejection by tryptophan catabolism. Science 281:1191–1193
Roy EJ, Takikawa O, Kranz DM, Browna AR, Thomas DL (2005) Neuronal localization of indoleamine 2,3-dioxygenase in mice. Neurosci Lett 387:95–99
Sedlmayr P, Blaschitz A, Wintersteiger R, Semlitsch M, Hammer A, MacKenzie CR, Walcher W, et al. (2002) Localization of indoleamine 2,3-dioxygenase in human female reproductive organs and the placenta. Mol Hum Reprod 8:385–391
Shimizu T, Nomiyama S, Hirata F, Hayaishi O (1978) Indoleamine 2,3-dioxygenase: purification and some properties. Biochem J 253:4700–4706
Swanson KA, Zheng Y, Heidler KM, Mizobuchi T, Wilkes DS (2004) CDllc cells modulate pulmonary immune responses by production of indoleamine 2,3-dioxygenase. Am J Respir Cell Mol Biol 30:311–318
Terness P, Bauer TM, Röse L, Dufter C, Watzlik A, Simon H, Opelz G (2002) Inhibition of allogeneic T cell proliferation by indoleamine 2,3-dioxygenase-expressing dendritic cells: mediation of suppression by tryptophan metabolites. J Exp Med 196: 447–457
Uyttenhove C, Pilotte L, Theate I, Stroobant V, Colau D, Parmentier N, Boon T, et al. (2003) Evidence for a tumoral immune resistance mechanism based on tryptophan degradation by indoleamine-2,3-dioxygenase. Nat Med 9:1269–1274
Yamazaki F, Kuroiwa T, Takikawa O, Kido R (1985) Human indolylamine 2,3-dioxygenase. Its tissue distribution, and characterization of the placental enzyme. Biochem J 230:635–638
Yoshida K, Urade Y, Tokuda M, Hayaishi O (1979) Induction of indoleamine 2,3-dioxygenase in mouse lung during virus infection. Proc Natl Acad Sci USA 76:4084–4086

The Journal of Histochemistry & Cytochemistry